

Separation and reconstruction of simultaneous source data via iterative rank reduction

Jinkun Cheng¹ and Mauricio D. Sacchi¹

ABSTRACT

We have developed a rank-reduction algorithm based on singular spectrum analysis (SSA) that is capable of suppressing the interferences generated by simultaneous source acquisition. We evaluated an inversion scheme that minimizes the misfit between predicted and observed blended data in t - x domain subject to a low-rank constraint that is applied to data in the f - x domain. In particular, we developed an iterative algorithm by adopting the projected gradient method with the SSA filter acting as the projection operator. This method entails extracting small patches of data from a common receiver gather and organizing the spatial data at a given monochromatic frequency into a Hankel matrix. For the ideal unblended data, Hankel matrices

extracted from the data are of low rank. The incoherent interferences in common-receiver domain caused by simultaneously fired shots increase the rank of the aforementioned Hankel matrices. Therefore, rank-reduction filtering is an effective way to annihilate source interferences while preserving the unblended signal. Through tests with synthetic examples, we found that the interference can be effectively suppressed by the proposed method. In addition, we found that the proposed algorithm can be modified to simultaneously cope with deblending and data recovery. A real survey acquired in the Gulf of Mexico was used to mimic a simultaneous-source acquisition with missing shot locations. The algorithm was able to recover the missing shot gathers from the blended acquisition with an improvement of the signal quality of approximately 12 dB.

INTRODUCTION

Simultaneous source acquisition techniques have been gaining popularity as a low-cost strategy to increase survey density. By allowing temporal overlap between closely fired sources, one can acquire multiple shots in a time-efficient fashion and thereby reduce the cost of seismic data acquisition (Silverman, 1979; Beasley et al., 1998; Stefani et al., 2007; Hampson et al., 2008). Early work on simultaneous source techniques focused on land acquisition via Vibroseis systems (Silverman, 1979). Different phase-encoding schemes have been introduced to eliminate the crosstalk noise that is generated by having multiple Vibroseis systems operating at the same time on different spatial positions (Bagaini, 2006). In marine seismic surveys, on the other hand, phase-encoding techniques are not applicable for impulsive sources such as airguns. In this case, the separation of simultaneous sources relies on source geometric distances and/or specific firing times schemes (Beasley et al., 1998; Abma and Ross, 2013). For instance, Stefani et al. (2007) and Hampson et al. (2008) propose to randomize firing times

to produce interferences that are incoherent in domains, such as common receiver gathers and common offset gathers.

Processing steps such as prestack time migration are considered as passive separation methods that can suppress source interfaces caused by simultaneous source acquisition in the migrated seismic image (Krey, 1987; Lynn et al., 1987). However, the latter might not be an optimal solution when performing amplitude-sensitive analysis on prestack data, such as amplitude variation with offset inversion and time-lapse seismic monitoring (Ayeni et al., 2011). For this reason, additional processing steps are often required to eliminate the interferences. One strategy entails converting source separation into an incoherent noise removal problem in common receiver gathers (Spitz et al., 2011; Ibrahim and Sacchi, 2013) or common offset gathers (Huo et al., 2009; Maraschini et al., 2012; Peng and Liu, 2013). For instance, one can adopt coherent pass operators including median filters, f - x prediction filters, and Radon transforms to suppress the incoherent interferences. Another family of methods treats source separation by solving an inverse problem. In this case, the data are transformed to auxiliary domains, in which constraints

Manuscript received by the Editor 15 August 2014; revised manuscript received 5 January 2015; published online 29 May 2015.

¹University of Alberta, Department of Physics, Edmonton, Alberta, Canada. E-mail: jinkun@ualberta.ca; msacchi@ualberta.ca.

© 2015 Society of Exploration Geophysicists. All rights reserved.

to eliminate incoherent interferences are effectively implemented by sparse inversion techniques (Akerberg et al., 2008; Moore et al., 2008; Lin and Herrmann, 2009; Abma et al., 2010; Mansour et al., 2012; Li et al., 2013; Chen et al., 2014). The latter is done in conjunction with the minimization of a misfit function to guarantee that the separated data reproduce the simultaneous source data. Compared with filtering techniques, deblending via inversion methods usually leads to better separation results (Moore, 2010; van Borselen et al., 2012).

Research on seismic signal processing via rank reduction techniques has been applied to signal-to-noise-ratio enhancement (Jones and Levy, 1987; Freire and Ulrych, 1988; Marchisio et al., 1988; Al-Yahya, 1991; Trickett, 2003; Chen and Sacchi, 2013) and, more recently, to the problem of seismic data reconstruction (Sacchi, 2009; Trickett and Burroughs, 2009; Oropeza and Sacchi, 2011). Rank-reduction methods for signal enhancement that are based on Cadzow filtering (Cadzow, 1988; Trickett and Burroughs, 2009) or singular spectrum analysis (SSA) filtering (Sacchi, 2009; Oropeza and Sacchi, 2011; Gao et al., 2013) are of special interest to this work. Cadzow or SSA filtering denotes a family of methods, where rank reduction is applied to Hankel matrices formed from noisy and often incomplete observations. These methodologies are found under different names in signal and image processing (Cadzow, 1988), time-series and spectral analysis (Vautard and Ghil, 1989; Hua, 1992), and dynamical systems (Broomhead and King, 1986). For instance, researchers in the field of time series analysis and dynamical systems frequently adopt the name SSA. On the contrary, researchers in the field of communications often use the name Cadzow's iterative denoising (Blu et al., 2008). In this paper, we will use the designation adopted by Sacchi (2009), Oropeza and Sacchi (2011), and Gao et al. (2013), and therefore, we will call our rank-reduction denoising method *SSA filtering*. We are aware, however, that equivalent denoising and reconstruction algorithms have been extensively studied in seismic data processing by Trickett and Burroughs (2009) who use the name *Cadzow filtering*.

Our main contribution is the introduction of the SSA reduced-rank filter in conjunction with an inversion scheme for suppressing interferences that arise in simultaneous source acquisition (Cheng

and Sacchi, 2013). The method is formulated in terms of a projected gradient optimization approach (Fazel, 2002; Meka et al., 2010), in which a cost function is minimized subject to a rank constraint. The rank constraint is imposed on small windows via the SSA filter.

PRELIMINARIES

A signal model for representing simultaneous source data

Seismic data acquired via a conventional seismic acquisition survey are denoted as $d(t, r, s)$, where t , r , and s are used to indicate the time, receiver, and source indices, respectively. The trace recorded by one receiver (r_j) by firing simultaneous sources is denoted by

$$b(t, r_j) = \sum_{k \in \mathbb{S}} d(t + \tau_k, r_j, s_k), \quad (1)$$

where \mathbb{S} indicates a group of shots with firing time and location pairs (τ_k, s_k) . For the j th receiver, the last expression can be written in operator form as follows:

$$\mathbf{b} = \mathcal{B}\mathbf{d}, \quad (2)$$

where \mathcal{B} symbolizes the blending operator (Berkhout, 2008), \mathbf{b} is the blended data, and \mathbf{d} denotes the ideal unblended common receiver gather for receiver j . Note that to avoid notational clutter, we drop the subindex j and understand that the proposed analysis is carried out for all receivers. In other words, equation 2 represents one detector j . The pseudo-deblended data are obtained by truncating and shifting samples of \mathbf{b} into a common receiver gather,

$$\hat{\mathbf{d}} = \mathcal{B}^*\mathbf{b}, \quad (3)$$

the operator \mathcal{B}^* denotes the pseudo-deblended operator that also turns out to be the adjoint of the operator \mathcal{B} (Berkhout, 2008; Mahdad et al., 2011).

Furthermore, we will decompose the ideal common receiver gather that one would have obtained via standard acquisition into small overlapping windows (Figure 1). We assume that each window is composed of a superposition of a finite number of linear dips. The synthesis of the data in terms of small windows is written as follows (Claerbout, 1997):

$$\mathbf{d} = \sum_{l=1}^L \mathcal{W}_l \mathbf{d}_l, \quad (4)$$

where \mathbf{d}_l is the l th data window and \mathcal{W}_l represents an operator that translates data windows with proper tapering in the areas where adjacent windows overlap. Similarly, we define an adjoint operator of the form

$$\mathbf{d}_l = \mathcal{W}_l^* \mathbf{d}, \quad l = 1, \dots, L, \quad (5)$$

where \mathcal{W}_l^* represents an operator that extracts the window l from the data with proper tapering in the areas where adjacent windows overlap. The operators \mathcal{W}_l and \mathcal{W}_l^* are written in explicit form, and special attention has been taken to guarantee

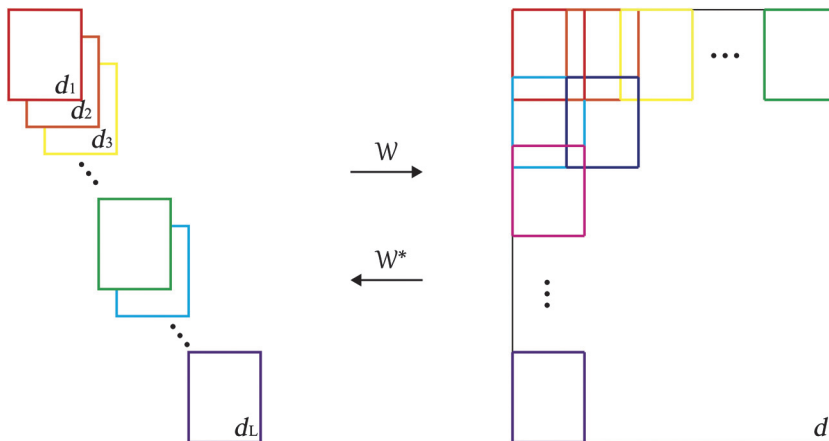


Figure 1. The windowing operator and its adjoint operator. The windowing operator \mathcal{W} extracts small patches of data from an entire gather. The adjoint operator \mathcal{W}^* combines all the processed small patches back into a gather. A cosine taper is used to combine areas with overlap.

that they pass the dot product test. The latter ensures that expressions 4 and 5 are a forward-adjoint pair (Claerbout, 1992). The aforementioned windowing strategy can be extended to multidimensional seismic data.

Reduced-rank filtering

We provide a short review of reduced-rank filtering for noise attenuation. The method can be found in the literature as Cadzow filtering or SSA. The details associated with the implementation of SSA for seismic noise attenuation and seismic data reconstruction can be found in Oropeza and Sacchi (2011). We discuss the 2D (t - x) implementation of reduced-rank filtering via SSA. However, we make the point that SSA for multidimensional volumes has been extensively discussed by Trickett et al. (2010), Oropeza and Sacchi (2011), and Gao et al. (2011). Seismic data in a small window can be represented in the frequency-space domain via the superposition of plane waves

$$D(\omega) = \sum_{k=1}^K A_k(\omega) e^{i\omega\eta_k j \Delta x}, \quad (6)$$

where $i = \sqrt{-1}$, $j = 1, 2, \dots, N$ is the trace index in the spatial axis, and ω represents temporal frequency. In this equation, we assume that the data are composed of K linear events with distinct dips η_k . We denote $A_k(\omega)$ as the complex amplitude of the k th plane wave, and Δx indicates the spatial interval between seismograms. The reduced-rank filtering method can be summarized as follows: We first construct a trajectory matrix by embedding complex amplitudes at one frequency $\mathbf{D}(\omega) = [D_1(\omega), D_2(\omega), \dots, D_N(\omega)]^T$ in the following Hankel matrix:

$$\begin{aligned} \mathbf{M}(\omega) &= \mathcal{H}[\mathbf{D}(\omega)] \\ &= \begin{bmatrix} D_1(\omega) & D_2(\omega) & \cdots & D_{N-L+1}(\omega) \\ D_2(\omega) & D_3(\omega) & \cdots & D_{N-L+2}(\omega) \\ \vdots & \vdots & \ddots & \vdots \\ D_L(\omega) & D_{L+1}(\omega) & \cdots & D_N(\omega) \end{bmatrix}, \end{aligned} \quad (7)$$

where the symbol \mathcal{H} is used to indicate the Hankel operator. For convenience, we choose $L = \lfloor \frac{N}{2} \rfloor + 1$ to make the Hankel matrix approximately square (Trickett and Burroughs, 2009; Oropeza and Sacchi, 2011), $\mathbf{M}(\omega) \in \mathbb{C}^{L \times (N-L+1)}$. We will omit the symbol ω and understand that the analysis is carried out for all frequencies. For a superposition of K plane waves, one can show that $\text{rank}(\mathbf{M}) = K$ (Hua, 1992; Yang and Hua, 1996). Additive noise in \mathbf{D} will increase the rank of matrix \mathbf{M} . Then, one can use rank reduction to attenuate the additive noise. The SSA filter can be represented via the following expression:

$$\mathbf{D}_F = \mathcal{A}[\mathcal{R}[\mathcal{H}[\mathbf{D}]]] = \mathcal{P}\mathbf{D}, \quad (8)$$

where \mathcal{A} is the antidiagonal averaging operator, \mathcal{R} is the rank-reduction operator that approximates \mathbf{M} by a rank- K matrix and \mathcal{H} is the Hankel operator. The operator \mathcal{A} transforms back a Hankel form into a vector by averaging across antidiagonals. Finally, the reduced-rank filter is summarized by the operator \mathcal{P} . Equation 8 represents the reduced-rank filtering in the frequency-space domain. For our analysis, it is more convenient to represent the SSA filter in the t - x domain

$$\mathbf{d}_F = \mathcal{F}^* \mathcal{A}[\mathcal{R}[\mathcal{H}\mathcal{F}[\mathbf{d}]]] = \mathcal{P}\mathbf{d}, \quad (9)$$

where \mathcal{F} and \mathcal{F}^* represent forward and inverse Fourier operators to transform data from the t - x domain to the f - x domain and from the f - x domain to the t - x domain, respectively. The operator \mathcal{P} represents the SSA rank-reduction filter that will be used by our source separation algorithm.

SOURCE SEPARATION VIA PROJECTED GRADIENTS METHOD

We assume that the ideal data before blending (common receiver gather) can be represented by the superposition of the t - x domain windows (equation 4). We also assume that each window is composed of a finite number of linear events. Therefore, in the f - x domain, the data lead to low-rank Hankel structures that were discussed in the preceding section. Combining equations 2 and 4 and after considering additive noise in the blended data,

$$\mathbf{b} = \mathcal{B} \sum_l \mathcal{W}_l \mathbf{d}_l + \mathbf{n}. \quad (10)$$

The separation of sources can be expressed as finding the solution of

$$\mathbf{d}_l = \underset{d_l}{\text{argmin}} \left\| \mathbf{b} - \mathcal{B} \sum_l \mathcal{W}_l \mathbf{d}_l \right\|_2^2, \quad l = 1, \dots, L. \quad (11)$$

Clearly, once $\mathbf{d}_l, l = 1, \dots, L$ are found, equation 11 is used to reconstruct the common receiver gather. However, the cost function (11) does not have a unique solution. Therefore, an additional constraint is needed to solve the problem. Our constraint is given by

$$\mathbf{d}_l = \mathcal{P}\mathbf{d}_l, \quad l = 1, \dots, L. \quad (12)$$

The problem is solved using a projected gradient method (Bertsekas, 1999). We define the gradient of equation 11 by

$$\mathbf{g}_l = \mathcal{W}_l^* \mathcal{B}^* \left(\mathcal{B} \sum_m \mathcal{W}_m \mathbf{d}_m - \mathbf{b} \right), \quad l, m = 1, \dots, L. \quad (13)$$

The projected gradient update rule can be written in the following way:

$$\begin{aligned} \mathbf{d}_l^{[\nu+1]} &= \mathcal{P} \left[\mathbf{d}_l^{[\nu]} - \lambda \mathcal{W}_l^* \mathcal{B}^* \left(\mathcal{B} \sum_m \mathcal{W}_m \mathbf{d}_m^{[\nu]} - \mathbf{b} \right) \right], \\ l, m &= 1, \dots, L, \end{aligned} \quad (14)$$

where ν denotes iteration number and $\lambda^{[\nu]}$ is the step size (Goldstein, 1964; Levitin and Polyak, 1966; Bertsekas, 1976). Similar iteration strategies have been used to deblend simultaneous sources by Cheng and Sacchi (2013), Peng and Liu (2013), and Chen et al. (2014).

In each iteration, we minimize the cost function by updating the solution in the gradient descent direction. The solutions are then projected to a set of low-rank matrices in the f - x domain. The projection operator \mathcal{P} separates the signal and the interferences, while preserving the ideal Hankel structure associated to each window. A similar algorithm, known as the fixed point iterative algorithm or singular value projection, has been discussed in the context of matrix completion by Meka et al. (2010), Ma et al. (2011), and Tanner and Wei (2013).

The projected gradient method intends to find the shortest distance, or the intersection of two closed sets: the set of minimum misfit and the set of the low-rank matrices. If both of the two sets were convex, the algorithm converges to the local optimal, which is also the global optimal of the cost function. In our case, due to the nonconvex nature of the set of low-rank matrices, it is difficult to prove the convergence of the algorithm to a global minimum. The iterative algorithm can be trapped into local minima if the initial point and step size are not properly selected (Fazel, 2002). However, Ma et al. (2011) has shown that the convergence of the fixed point algorithm can be guaranteed when

$$\lambda^{[0]} < 2/\sigma_{\max}, \quad (15)$$

where σ_{\max} is the maximum eigenvalue of the operator $\mathcal{B}^*\mathcal{B}$. In this paper, a reasonable candidate for the initial solution is the pseudo-deblended data. This is because the pseudo-deblended data contain

exactly the desired common receiver gather and is likely close to the true solution. Convergence can be achieved by equation 15 and diminishing step lengths (Bertsekas, 1999; Nedic and Bertsekas, 2001). In the example, the step size is decreased according to $\lambda^{[v]} = \lambda^{[0]}/\sqrt{v}$. Our selection of step size guarantees the convergence. However, there might be other step-size schedules that might speed up the convergence of the algorithm (Mahdad et al., 2011).

Joint separation and reconstruction of seismic sources

We turn our attention to the case in which the seismic data are not regularly sampled in the source coordinate. In other words, we assume that some sources were not fired. The aforementioned source separation algorithm will encounter problems because our f - x domain model is effective only when the sources satisfy a regular spatial distribution. However, the data in the unblended domain can be approximated as the entrywise product of the complete data set and a sampling operator \mathcal{T} . The operator \mathcal{T} multiplies traces that are alive by 1, whereas dead traces are multiplied by 0 (Sacchi and Liu, 2005). Without losing generality, the new problem is solved via

$$\mathbf{d}_l = \operatorname{argmin}_{\mathbf{d}_l} \left\| \mathbf{b} - \mathcal{B}\mathcal{T} \sum_l \mathcal{W}_l \mathbf{d}_l \right\|_2^2, \quad (16)$$

$$l = 1, \dots, L.$$

Therefore, the projected gradient method turns into

$$\mathbf{d}_l^{[v+1]} = \mathcal{P} \left[\mathbf{d}_l^{[v]} - \lambda \mathcal{W}_l^* \mathcal{T}^* \mathcal{B}^* \left(\mathcal{B}\mathcal{T} \sum_m \mathcal{W}_m \mathbf{d}_m^{[v]} - \mathbf{b} \right) \right], \quad (17)$$

$$l, m = 1, \dots, L,$$

where it is easy to show that $\mathcal{T} = \mathcal{T}^*$ and $\mathcal{T}^*\mathcal{T} = \mathcal{T}$ (Liu and Sacchi, 2004; Naghizadeh and Sacchi, 2010).

EXAMPLES

Comparison of projection operators

To test the performance of the proposed deblending method, we first synthesize an example with three crossing linear events to mimic a small patch of a noise-free common receiver gather (Figure 2a). We then introduce severe blending noise (Figure 2b). In addition to source separation via the proposed iterative rank reduction approach, we also test the iterative f - x deconvolution method and the iterative f - k thresholding algorithm. In other words, we replace the rank-reduction operator \mathcal{P} in equation 14 by an f - x deconvolution operator (Peng and Liu, 2013) and by the f - k hard-thresholding operator (Abma et al., 2010; Chen et al., 2014).

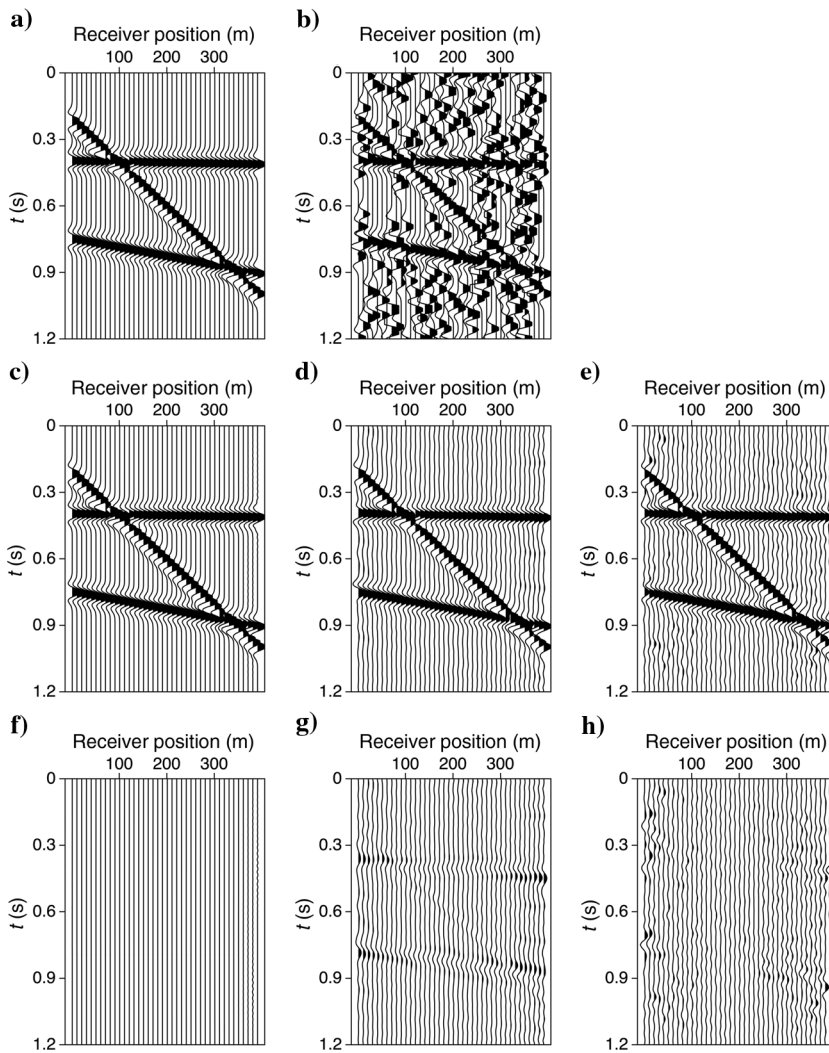


Figure 2. Comparisons of deblending results for numerically blended synthetic data with linear events. (a) The original unblended synthetic data, (b) pseudo-deblended gather, (c) deblending result with the proposed iterative rank reduction method, (d) deblending result using iterative f - x deconvolution, (e) deblending results using iterative f - k domain thresholding, (f) difference section between panels (a) and (c), (g) difference section between panels (a) and (d), and (h) difference section between panels (a) and (e).

We adopt a rank $K = 3$ for each iteration for the iterative rank reduction deblending method. The f - x deconvolution is implemented with a 15-point filter. As to the f - k domain thresholding method, we adopt the exponential schedule proposed by Gao et al. (2010) to slowly decrease the amplitude threshold. We also tune the step size to make sure that the three methods follow similar convergence curves. The qualities of pseudo-deblending Q_{PD} and deblending Q_S are calculated in dB units via the following two expressions:

$$Q_{PD} = 10 \log \frac{\|d_{true}\|_2^2}{\|d_{true} - d_{PD}\|_2^2}, \quad Q_S = 10 \log \frac{\|d_{true}\|_2^2}{\|d_{true} - d_S\|_2^2}, \quad (18)$$

Table 1. Quality of source separation Q_S and performance I for the iterative projected gradient method for different projection operators: rank reduction (proposed method), f - x deconvolution (Peng and Liu, 2013), and f - k thresholding (Abma et al., 2010). These results correspond to the comparison tests portrayed in Figure 2.

Projection	Q_S (dB)	$I = Q_S - Q_{PD}$ (dB)
Rank reduction	20.2	22.5
f - x deconvolution	10.1	12.4
f - k thresholding	12.0	14.3

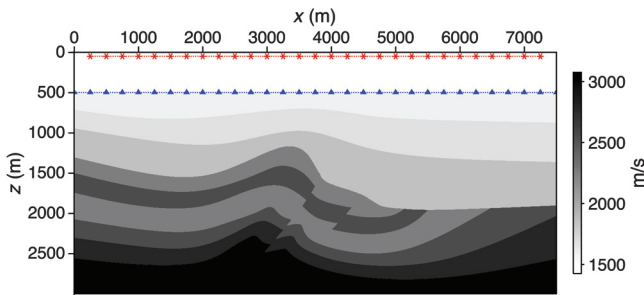


Figure 3. Velocity model used to simulate blended data for our examples via finite-difference modeling. We synthesize a data set with a 4-ms time interval and a 20-Hz central-frequency Ricker wavelet. We also overlaid the source (*) and receiver (▲) geometry in this plot.

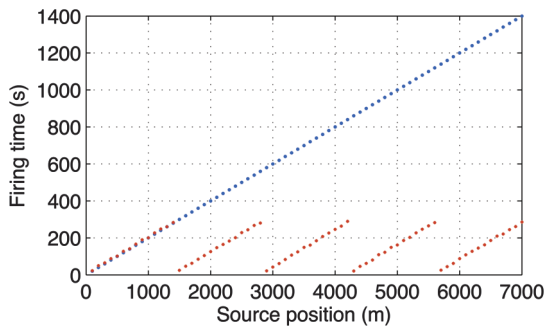


Figure 4. Spatial and temporal distribution of firing times for conventional seismic acquisition (blue) and 2D simultaneous source acquisition (every fifth shot). The multivessel scenario is portrayed in red. In each round, five sources fire with small random time delays. The spatial distance between sources is fixed in each round.

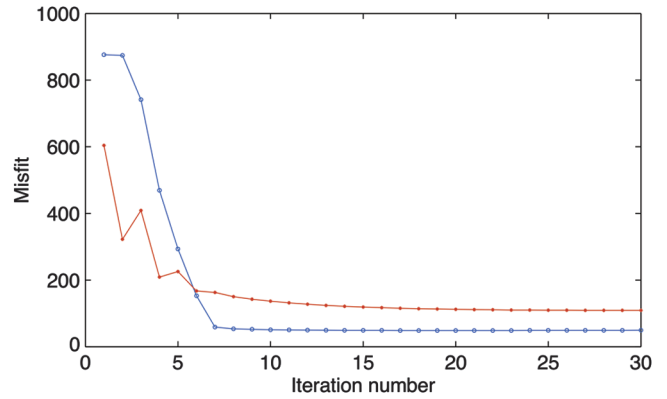


Figure 5. Convergence of the iterative rank-reduction source-separation algorithm. The blue line indicates the l_2 -norm of the difference between blended observations and the synthesized blended observation versus iteration. We also portray in red the difference between the unblended data and the true data versus iteration.

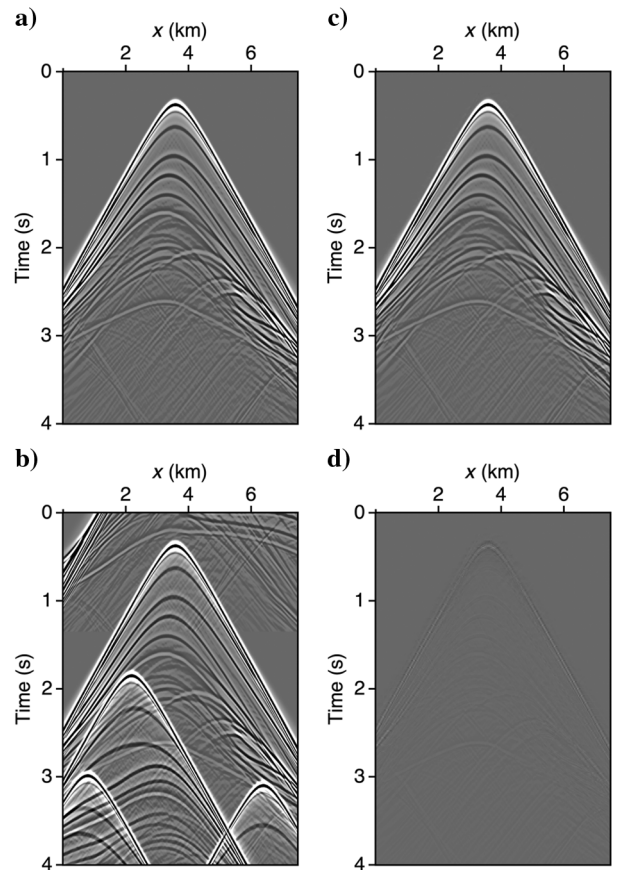


Figure 6. Results of the proposed iterative rank-reduction deblending method in the common-shot domain. (a) The original shot gather from synthetic data, (b) pseudo-deblended shot gather after numerical blending, (c) the deblended shot gather after 30 iterations of the proposed algorithm. The quality of data has been improved to 15.1 dB with respect to 0.5 dB, and (d) difference section between original and deblended data.

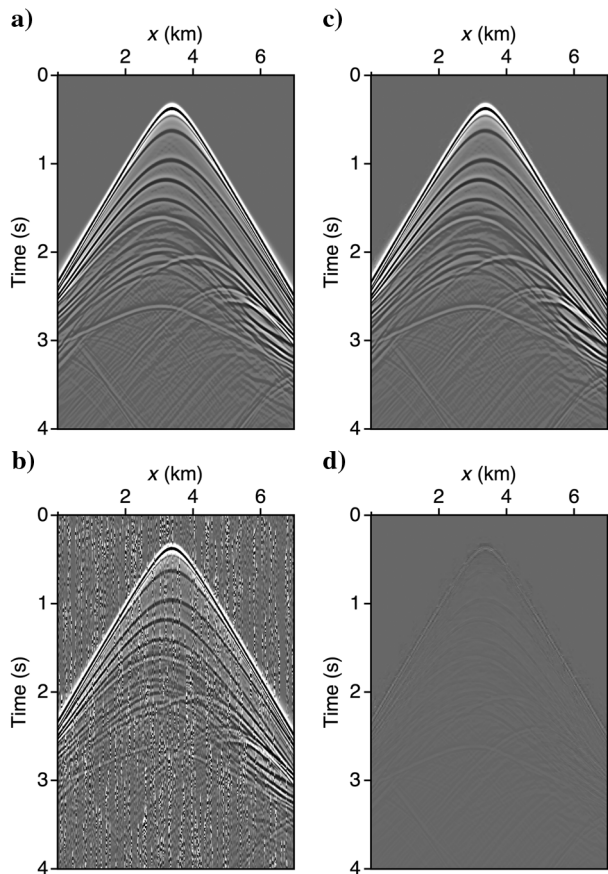
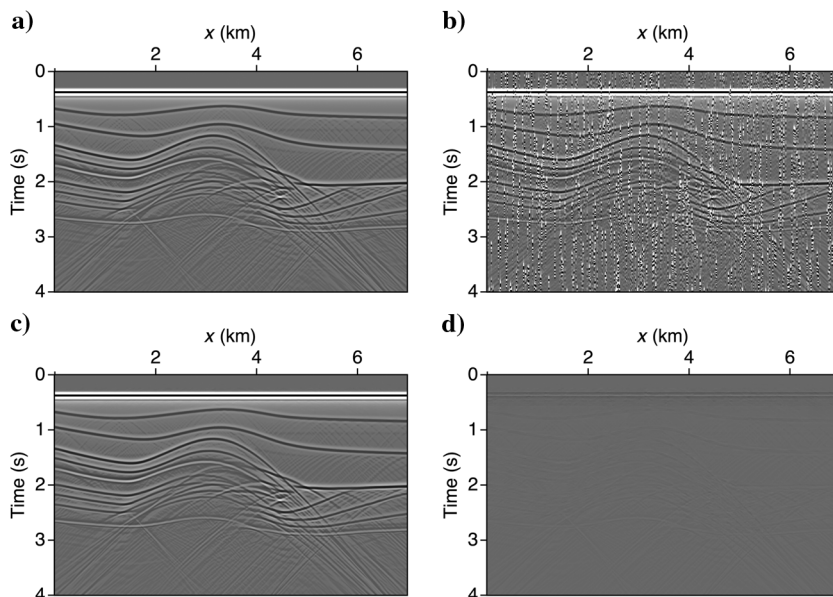


Figure 7. Results of the proposed iterative rank-reduction deblending method in the common-receiver domain. (a) The original common receiver gather from synthetic data, (b) pseudo-deblended common receiver gather after numerical blending, (c) the deblended common receiver gather after 30 iterations of the proposed method. The quality of data has been improved to 15.1 dB with respect to 0.5 dB, and (d) difference section between original and deblended data.

Figure 8. Results of the proposed iterative rank-reduction deblending method for the near-offset section. (a) The original near-offset section from synthetic data, (b) pseudo-deblended near-offset section after numerical blending, (c) the deblended near-offset section after 30 iterations. The quality of data has been improved to 15.1 dB with respect to 0.5 dB, and (d) difference section between original and deblended data.



where d_{PD} denotes the pseudo-deblended common receiver gather, d_{true} is the true synthetic data (a conventional common receiver gather), and d_S stands for the separated common receiver gather via the iterative projected gradient algorithm. A large Q value corresponds to fewer interferences. The performance of the method is given by $I = Q_S - Q_{PD}$.

Figure 2f shows the deblended data obtained via the proposed iterative rank-reduction method. Figure 2f shows the difference section for the iterative rank-reduction method. Figure 2d and 2g portray the deblended data, and the difference section for the projected gradient algorithm with projection operator given by f - x deconvolution, respectively. Similarly, Figure 2e and 2h shows the deblended data, and the difference section for the projected gradient algorithm with projection operator given by f - k thresholding. For completeness, we have added Table 1 to indicate Q_S and I for our examples ($Q_{PD} = -2.3$ dB). Our results indicate that for this particular example, rank reduction provides the highest attenuation of source interference noise. This should not come as a surprise to us; three linear events can be optimally modeled via a Hankel matrix of rank 3.

Synthetic example for simultaneous source separation

We also test the proposed deblending algorithm with a 2D synthetic example. In this example, we use an acoustic finite-difference modeling code to simulate a prestack marine data set. The velocity model as well as the source and receiver geometry are shown in Figure 3. The sources and receivers are distributed every 20 m. A total of 350 sources were simulated. Each source fires into a fixed array of 375 receivers. The receivers are deployed at a 500-m depth to simulate ocean-bottom nodes.

We use groups of five shots with fixed spacing (1400 m) that were blended with time intervals generated from uniform distribution from 0 to 2 s. Then, all the five sources moved to the next position and are blended again. A total of 70 blended shots were generated. Figure 4 shows the spatial and temporal distribution of sources for this particular acquisition. As a result, the total acquisition time was compressed to 20% of the conventional acquisition time. Then, we apply the proposed algorithm to recover the common receiver gathers

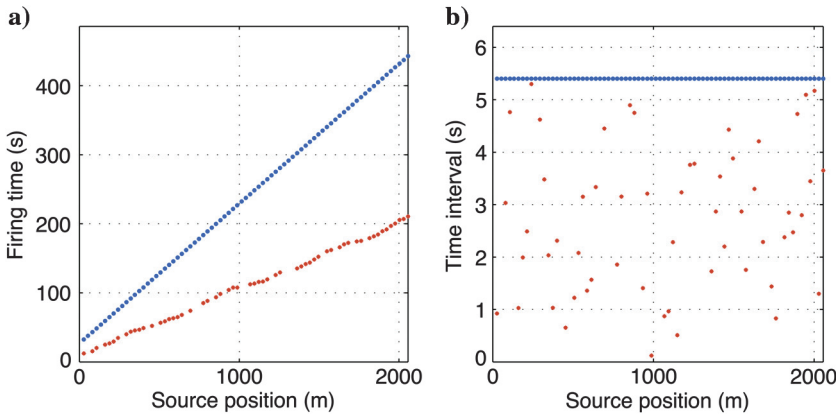


Figure 9. Spatial and temporal distribution of firing time for a conventional seismic acquisition (blue) and 2D simultaneous source acquisition with 25 missing shots for one-vessel scenario (red). (a) Source firing times and (b) firing time intervals between adjacent sources.

and to form separated source gathers for the whole volume. The operator \mathcal{W} extracts windows of size 100 samples in time and 40 traces. The overlap is of 25 samples in time and 10 traces in space. A cosine taper was applied in time and space.

Figure 5 shows the misfit between the solution and the observed blended data for one receiver. The curve also shows the difference between the solution at a given iteration versus the true answer. The algorithm is comparatively effective as both curves reach convergence after approximately 15 iterations. The misfit did not reduce to zero due to the strategy we adopt for selecting the rank. It is important to mention that for each window, we let the rank of the SSA filter increase with iterations. At early iterations, we can apply harsh filtering to eliminate strong crosstalk and then, gradually increase the rank to allow retrieving details that depart from the linear event model. This is analogous to setting the threshold

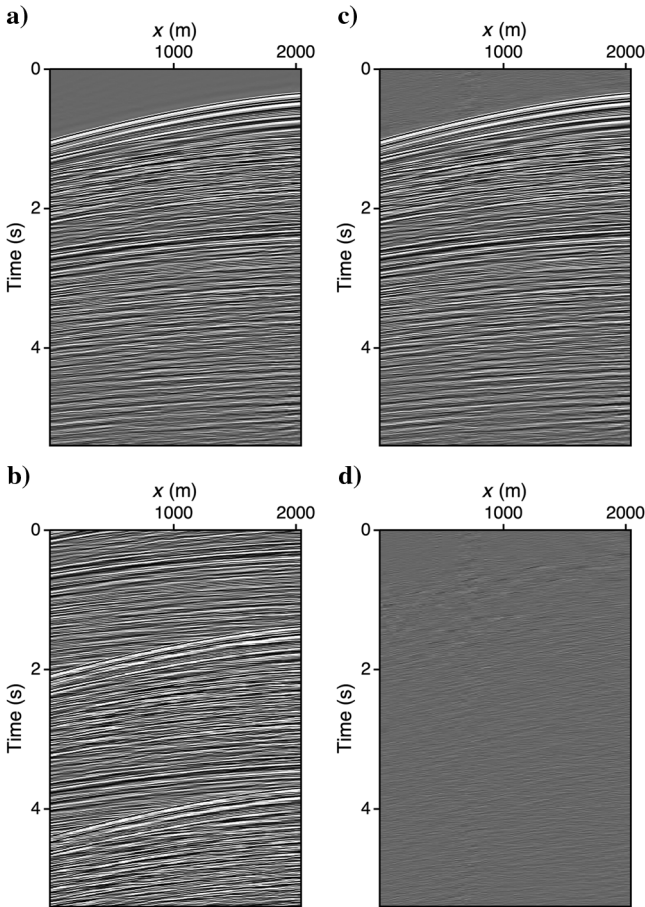


Figure 10. Results of deblending and reconstruction for a common shot gather. (a) The original shot gather from the Gulf of Mexico data set, (b) pseudo-deblended shot gather after numerical blending and sampling. The desired source is missing, (c) the deblended and reconstructed shot gather after 30 iterations. The quality of data has been improved to 10.8 dB from -1.5 dB, and (d) difference section between the original and deblended and reconstructed data.

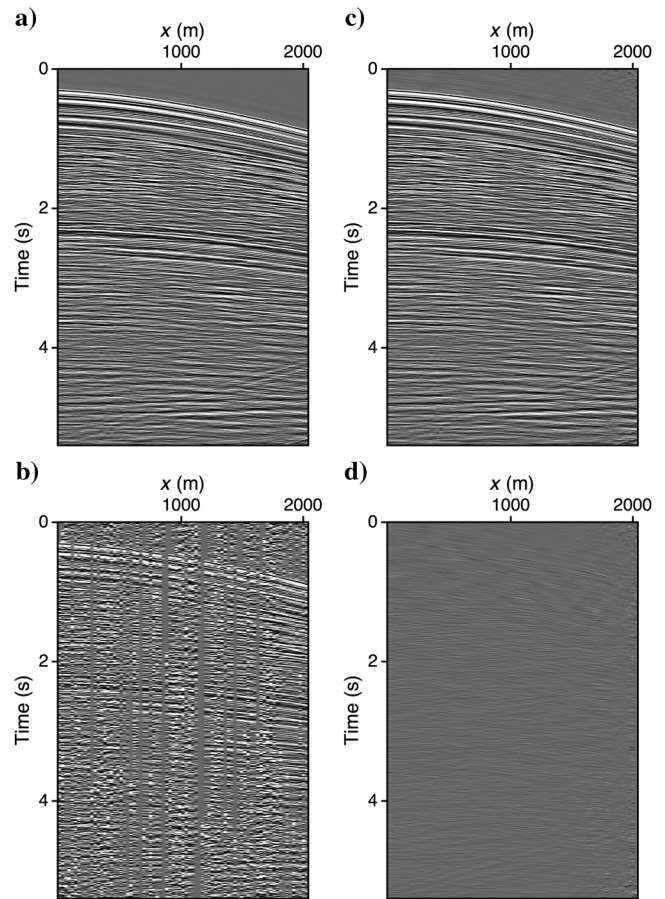


Figure 11. Results of deblending and reconstruction for a common receiver gather. (a) The original common receiver gather from the Gulf of Mexico data set, (b) pseudo-deblended common receiver gather after numerical blending, (c) the deblended common receiver gather after 30 iterations. The quality of data has been improved to 10.8 dB from -1.5 dB, and (d) difference section between original and deblended data.

schedule in projection-onto-convex sets interpolation and deblending methods (Abma et al., 2010).

We carried out a large number of simulations to determine rank selection schedules. A strategy that works for us entails starting with a small rank $k = 3$ and then increasing the rank by one in every five iterations. In short, the final rank for our example after 30 iterations is $k = 9$. Figures 6 and 7 show the results of the separation after 30 iterations for shot and receiver number 175. In this example, the proposed algorithm improved the quality from 0.5 dB to a factor of 15.1 dB ($I = 14.6$ dB). The unblended solution becomes comparable with the true conventional data set. Figure 8 shows the near-offset section for this data set. The interferences from simultaneously fired shots are effectively suppressed. It is important to note that high-amplitude direct waves can severely affect the performance of the algorithm. In fact, the proposed rank-reduction algorithm is suited for scenarios in which the direct waves are not extremely strong. This is consistent with the results presented by Maraschini et al. (2012).

Joint simultaneous source separation and reconstruction

We use a conventional data set collected from the Gulf of Mexico to simulate a blended acquisition. To synthesize the blending acquisition, we assume a self-simultaneous source scenario with one

vessel firing. The receivers are ocean-bottom nodes. Because the air-gun sources are impulsive, the vessel keeps traveling without waiting for the recordings. Under this scenario, random fire time delays usually lead to an irregular distribution of source positions. This problem is tackled by moving the exact source position to the nearest grid point (Li et al., 2013). In this example, the spatial and temporal sampling intervals are set to be 26.6 m and 4 ms, respectively. As is shown in Figure 9, the firing time intervals between adjacent sources follow a uniform distribution. The overall acquisition time is reduced by 50%. We consider the case in which 25 out of a total number of 80 sources are missing in an irregular pattern. Figure 10 shows a common shot gather recovered after 30 iterations. Note that we intentionally pick a common shot gather with the desired source missing. The pseudo-deblended shot gather only contains interferences from nearby sources. Figure 11 shows the deblended common receiver gather; the quality of the reconstruction has been improved to $Q_S = 10.8$ dB with respect to $Q_{PD} = -1.5$ dB ($I = 12.3$ dB). We also display the whole volume for this small data set in Figure 12. Unfortunately, the low fold of this example precludes us displaying a realistic near-offset section.

CONCLUSION

This paper illustrates an iterative rank-reduction algorithm based on SSA filtering for separating and reconstructing simultaneous source data. The proposed algorithm can be classified among the family of deblending methods via inversion. By implementing rank reduction with a projection operator, the SSA filter, solutions are constrained to be low rank in Hankel matrices extracted from small spatial-temporal windows in common receiver gathers. The latter is important because the SSA method is a valid denoising and reconstruction technique for a superposition of plane waves. In a small window, the data can be approximated via a limited number of dips plus incoherent interferences caused by the blending process. Convergence of this algorithm can be achieved if the pseudo-deblended data are adopted as the initial solution. Through tests with synthetic examples made by blending a traditional marine acquisition, we show that the interferences of the wavefields can be effectively suppressed. At the same time, we can reconstruct the missing seismic sources. The latter offers more freedom from the perspective of acquisition design for simultaneous source methods. One can start to analyze source separation in conjunction with seismic data reconstruction as two problems that can be simultaneously attacked to optimize the ubiquitous quality-cost trade-off. This algorithm could also see applications in multidimensional cases by adopting high-order SVD or tensor-based dimensionality reduction methods.

ACKNOWLEDGMENTS

The authors wish to thank the sponsors of the Signal Analysis and Imaging Group at the Department of Physics of the University of Alberta

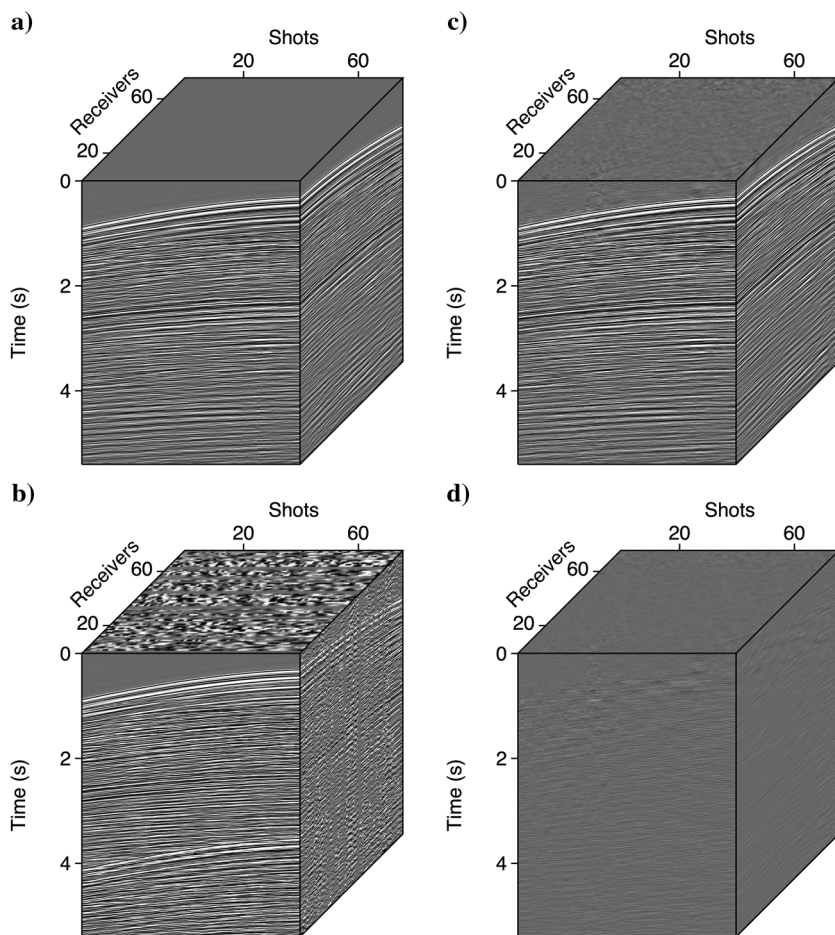


Figure 12. Results of deblending and reconstruction for the whole data volume. (a) The original data from the Gulf of Mexico, (b) pseudo-deblended data, (c) the deblended data after 30 iterations, and (d) difference section between original and deblended data.

for supporting this research. We also thank the associate editor A. Baumstein and three anonymous reviewers for their valuable suggestions that improved the manuscript.

REFERENCES

- Abma, R., T. Manning, M. Tanis, J. Yu, and M. Foster, 2010, High quality separation of simultaneous sources by sparse inversion: 72nd Annual International Conference and Exhibition, EAGE, Extended Abstracts, B003.
- Abma, R., and A. Ross, 2013, Popcorn shooting: Sparse inversion and the distribution of airgun array energy over time: 83rd Annual International Meeting, SEG, Expanded Abstracts, 31–35.
- Akerberg, P., G. Hampson, J. Rickett, H. Martin, and J. Cole, 2008, Simultaneous source separation by sparse Radon transform: 78th Annual International Meeting, SEG, Expanded Abstracts, 2801–2085.
- Al-Yahya, K., 1991, Application of the partial Karhunen-Loève transform to suppress random noise in seismic sections: *Geophysical Prospecting*, **39**, 77–93, doi: [10.1111/j.1365-2478.1991.tb00302.x](https://doi.org/10.1111/j.1365-2478.1991.tb00302.x).
- Ayeni, G., A. Almonmin, and D. Nichols, 2011, On the separation of simultaneous-source data by inversion: 81st Annual International Meeting, SEG, Expanded Abstracts, 20–25.
- Bagaini, C., 2006, Overview of simultaneous Vibroseis acquisition methods: 76th Annual International Meeting, SEG, Expanded Abstracts, 70–74.
- Beasley, C. J., R. E. Chambers, and Z. Jiang, 1998, A new look at simultaneous sources: 68th Annual International Meeting, SEG, Expanded Abstracts, 133–135.
- Berkhout, A. J., 2008, Changing the mindset in seismic data acquisition: *The Leading Edge*, **27**, 924–938, doi: [10.1190/1.2954035](https://doi.org/10.1190/1.2954035).
- Bertsekas, D. P., 1976, On the Goldstein-Levitin-Polyak gradient projection method: *IEEE Transactions on Automatic Control*, **21**, 174–184, doi: [10.1109/CDC.1974.270399](https://doi.org/10.1109/CDC.1974.270399).
- Bertsekas, D. P., 1999, *Nonlinear programming*: Athena Scientific.
- Blu, T., P.-L. Dragotti, M. Vetterli, P. Marziliano, and L. Coulot, 2008, Sparse sampling of signal innovations: *IEEE Signal Processing Magazine*, **25**, 31–40, doi: [10.1109/MSP.2007.914998](https://doi.org/10.1109/MSP.2007.914998).
- Broomhead, D., and G. King, 1986, Extracting qualitative dynamics from experimental data: *Physica D*, **20**, 217–236, doi: [10.1016/0167-2789\(86\)90031-X](https://doi.org/10.1016/0167-2789(86)90031-X).
- Cadzow, J., 1988, Signal enhancement—a composite property mapping algorithm: *IEEE Transactions on Acoustics, Speech and Signal Processing*, **36**, 49–62, doi: [10.1109/29.1488](https://doi.org/10.1109/29.1488).
- Chen, K., and M. D. Sacchi, 2013, Robust reduced-rank seismic denoising: 83rd Annual International Meeting, SEG, Expanded Abstracts, 4272–4277.
- Chen, Y., S. Fomel, and J. Hu, 2014, Iterative deblending of simultaneous-source seismic data using seislet-domain shaping regularization: *Geophysics*, **79**, no. 5, V179–V189, doi: [10.1190/geo2013-0449.1](https://doi.org/10.1190/geo2013-0449.1).
- Cheng, J., and M. D. Sacchi, 2013, Separation of simultaneous source data via iterative rank reduction: 83rd Annual International Meeting, SEG, Expanded Abstracts, 88–93.
- Claerbout, J. F., 1992, *Earth soundings analysis: Processing versus inversion*: Blackwell Scientific Publications.
- Claerbout, J. F., 1997, Nonstationarity and conjugacy: Utilities for data patch work: *Stanford Exploration Project* 73, 391–400.
- Fazel, M., 2002, *Matrix rank minimization with applications*: Master's thesis, Stanford University.
- Freire, S., and T. Ulrych, 1988, Application of singular value decomposition to vertical seismic profiling: *Geophysics*, **53**, 778–785, doi: [10.1190/1.1442513](https://doi.org/10.1190/1.1442513).
- Gao, J., X. Chen, J. Li, and J. Ma, 2010, Irregular seismic data reconstruction based on exponential threshold model of POCS method: *Applied Geophysics*, **7**, 229–238, doi: [10.1007/s11770-010-0246-5](https://doi.org/10.1007/s11770-010-0246-5).
- Gao, J., M. Sacchi, and X. Chen, 2011, A fast rank reduction method for the reconstruction of 5D seismic volumes: 81st Annual International Meeting, SEG, Expanded Abstracts, 3622–3627.
- Gao, J., M. D. Sacchi, and X. Chen, 2013, A fast reduced-rank interpolation method for prestack seismic volumes that depend on four spatial dimensions: *Geophysics*, **78**, no. 1, V21–V30, doi: [10.1190/geo2012-0038.1](https://doi.org/10.1190/geo2012-0038.1).
- Goldstein, A. A., 1964, Convex programming in Hilbert space: *Bulletin of the American Mathematical Society*, **70**, 709–710, doi: [10.1090/S0002-9904-1964-11178-2](https://doi.org/10.1090/S0002-9904-1964-11178-2).
- Hampson, G., J. Stefani, and F. Herkenhoff, 2008, Acquisition using simultaneous sources: *The Leading Edge*, **27**, 918–923, doi: [10.1190/1.2954034](https://doi.org/10.1190/1.2954034).
- Hua, Y., 1992, Estimating two-dimensional frequencies by matrix enhancement and matrix pencil: *IEEE Transactions on Signal Processing*, **40**, 2267–2280, doi: [10.1109/78.157226](https://doi.org/10.1109/78.157226).
- Huo, S., Y. Luo, and P. Kelamis, 2009, Simultaneous sources separation via multi-directional vector-median filter: 79th Annual International Meeting, SEG, Expanded Abstracts, 150–173.
- Ibrahim, A., and M. D. Sacchi, 2014, Simultaneous source separation using a robust Radon transform: *Geophysics*, **79**, no. 1, V1–V11, doi: [10.1190/geo2013-0168.1](https://doi.org/10.1190/geo2013-0168.1).
- Jones, I., and S. Levy, 1987, Signal to noise ratio enhancement in multichannel seismic data via the Karhunen-Loève transform: *Geophysical Prospecting*, **35**, 12–32, doi: [10.1111/j.1365-2478.1987.tb00800.x](https://doi.org/10.1111/j.1365-2478.1987.tb00800.x).
- Krey, T. C., 1987, Attenuation of random noise by 2-D and 3-D CDP stacking and Kirchhoff migration: *Geophysical Prospecting*, **35**, 135–147, doi: [10.1111/j.1365-2478.1987.tb00809.x](https://doi.org/10.1111/j.1365-2478.1987.tb00809.x).
- Levitin, E. S., and B. T. Polyak, 1966, Constrained minimization methods: *USSR Computational Mathematics and Mathematical Physics*, **6**, 1–50, doi: [10.1016/0041-5553\(66\)90114-5](https://doi.org/10.1016/0041-5553(66)90114-5).
- Li, C., C. C. Mosher, L. C. Morley, Y. Ji, and J. D. Brewer, 2013, Joint source deblending and reconstruction for seismic data: 83rd Annual International Meeting, SEG, Expanded Abstracts, 82–87.
- Lin, T., and F. J. Herrmann, 2009, Designing simultaneous acquisitions with compressive sensing: 71st Annual International Conference and Exhibition, EAGE, Extended Abstracts, S006.
- Liu, B., and M. Sacchi, 2004, Minimum weighted norm interpolation of seismic records: *Geophysics*, **69**, 1560–1568, doi: [10.1190/1.1836829](https://doi.org/10.1190/1.1836829).
- Lynn, W., M. Doyle, L. Larner, and R. Marschall, 1987, Experimental investigation of interference from other seismic crews: *Geophysics*, **52**, 1501–1524, doi: [10.1190/1.1442268](https://doi.org/10.1190/1.1442268).
- Ma, S., D. Goldfarb, and L. Chen, 2011, Fixed point and Bregman method for matrix rank minimization and matrix completion: *Mathematical Programming Series A*, **128**, 321–353, doi: [10.1007/s10107-009-0306-5](https://doi.org/10.1007/s10107-009-0306-5).
- Mahdad, A., P. Doulgeris, and G. Blacquiere, 2011, Separation of blended data by iterative estimation and subtraction of blending interference noise: *Geophysics*, **76**, no. 3, Q9–Q17, doi: [10.1190/1.3556597](https://doi.org/10.1190/1.3556597).
- Mansour, H., H. Wason, T. Lin, and F. J. Herrmann, 2012, Randomized marine acquisition with compressive sensing: *Geophysical Prospecting*, **60**, 648–662, doi: [10.1111/j.1365-2478.2012.01075.x](https://doi.org/10.1111/j.1365-2478.2012.01075.x).
- Maraschini, M., R. Dyer, K. Stevens, and D. Bird, 2012, Source separation by iterative rank reduction — Theory and applications: 72nd Annual International Conference and Exhibition, EAGE, Extended Abstracts, A044.
- Marchisio, G., J. Pendrel, and B. Mattocks, 1988, Applications of full and partial Karhunen-Loève transformation to geophysical image enhancement: 58th Annual International Meeting, SEG, Expanded Abstracts, 1266–1269.
- Meka, R., P. Jain, and I. Dhillon, 2010, Guaranteed rank minimization via singular value projection: *Neural Information Processing Systems Conference*.
- Moore, I., 2010, Simultaneous sources — Processing and applications: Presented at 72nd Annual International Conference and Exhibition, EAGE, Extended Abstracts, B001.
- Moore, I., B. Dragoset, T. Ommundsen, D. Wilson, C. W., and D. Eke, 2008, Simultaneous source separation using dithered sources: 78th Annual International Meeting, SEG, Expanded Abstracts, 2806–2810.
- Naghizadeh, M., and M. D. Sacchi, 2010, On the sampling functions and Fourier reconstruction methods: *Geophysics*, **75**, no. 3, B137–B146, doi: [10.1190/1.3420735](https://doi.org/10.1190/1.3420735).
- Nedic, A., and D. P. Bertsekas, 2001, Incremental subgradient methods for nondifferentiable optimization: *SIAM Journal on Optimization*, **12**, 109–138., doi: [10.1137/S1052623499362111](https://doi.org/10.1137/S1052623499362111).
- Oropeza, V., and M. Sacchi, 2011, Simultaneous seismic data denoising and reconstruction via multichannel singular spectrum analysis: *Geophysics*, **76**, no. 3, V25–V32, doi: [10.1190/1.3552706](https://doi.org/10.1190/1.3552706).
- Peng, C., and B. Liu, 2013, Deblending of simultaneous sources using an iterative approach: An experiment with variable-depth streamer data: 83rd Annual International Meeting, SEG, Expanded Abstracts, 4278–4282.
- Sacchi, M. D., 2009, F-X singular spectrum analysis: Presented at CSPG CSEG CWLS Convention, 392–395.
- Sacchi, M. D., and B. Liu, 2005, Minimum weighted norm wavefield reconstruction for AVA imaging: *Geophysical Prospecting*, **53**, 787–801, doi: [10.1111/j.1365-2478.2005.00503.x](https://doi.org/10.1111/j.1365-2478.2005.00503.x).
- Silverman, D., 1979, Method of three dimensional seismic prospecting: U.S. Patent 4,159,463.
- Spitz, S., G. Hampson, and A. Pica, 2011, Simultaneous source separation: A prediction-subtraction approach: 81st Annual International Meeting, SEG, Expanded Abstracts, 2811–2815.
- Stefani, J., G. Hampson, and E. Herkenhoff, 2007, Acquisition using simultaneous sources: 69th Annual International Conference and Exhibition, EAGE, Extended Abstracts, B006.
- Tanner, J., and K. Wei, 2013, Normalized iterative hard thresholding for matrix completion: *SIAM Journal on Scientific Computing*, **35**, S104–S125, doi: [10.1137/120876459](https://doi.org/10.1137/120876459).
- Trickett, S. R., 2003, F-xy eigenimage noise suppression: *Geophysics*, **68**, 751–759, doi: [10.1190/1.1567245](https://doi.org/10.1190/1.1567245).

- Trickett, S. R., and L. Burroughs, 2009, Prestack rank-reducing noise suppression: 79th Annual International Meeting, SEG, Expanded Abstracts, 3332–3336.
- Trickett, S., L. Burroughs, A. Milton, L. Walton, and R. Dack, 2010, Rank-reduction-based trace interpolation: 80th Annual International Meeting, SEG, Expanded Abstracts, 3829–3833.
- Van Borselen, R., R. Baardman, T. Martin, B. Goswami, and E. Fromyr, 2012, An inversion approach to separating sources in marine simultaneous shooting acquisition — Application to a Gulf of Mexico data set: *Geophysical Prospecting*, **60**, 640–647, doi: [10.1111/j.1365-2478.2012.01076.x](https://doi.org/10.1111/j.1365-2478.2012.01076.x).
- Vautard, R., and M. Ghil, 1989, Singular spectrum analysis in non linear dynamics, with applications to paleoclimatic time series: *Physica D*, **35**, 395–424, doi: [10.1016/0167-2789\(89\)90077-8](https://doi.org/10.1016/0167-2789(89)90077-8).
- Yang, H. H., and Y. Hua, 1996, On rank of block Hankel matrix for 2-D frequency detection and estimation: *IEEE Transactions on Signal Processing*, **44**, 1046–1048., doi: [10.1109/78.492568](https://doi.org/10.1109/78.492568).